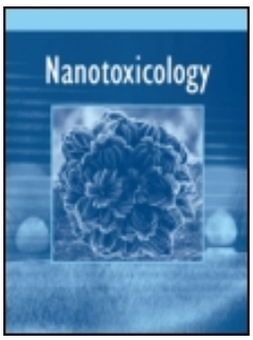

Nanotoxicology

ISSN: 1743-5390 (Print) 1743-5404 (Online) Journal homepage: https://www.tandfonline.com/loi/inan20

Toxicity and biodistribution of aqueous synthesized ZnS and ZnO quantum dots in mice

Yanjie Yang, Jingfeng Lan, Zhigang Xu, Tong Chen, Tong Zhao, Ting Cheng, Jianmin Shen, Shuangyu Lv & Haixia Zhang

To cite this article: Yanjie Yang, Jingfeng Lan, Zhigang Xu, Tong Chen, Tong Zhao, Ting Cheng, Jianmin Shen, Shuangyu Lv & Haixia Zhang (2014) Toxicity and biodistribution of aqueous synthesized ZnS and ZnO quantum dots in mice, Nanotoxicology, 8:1, 107-116, DOI: 10.3109/17435390.2012.760014

To link to this article: https://doi.org/10.3109/17435390.2012.760014

Nanotoxicology, February 2014; 8(1):107–116
© 2014 Informa UK, Ltd.
ISSN: 1743-5390 print / 1743-5404 online
DOI: 10.3109/17435390.2012.760014

informa
healthcare

Toxicity and biodistribution of aqueous synthesized ZnS and ZnO quantum dots in mice

Yanjie Yang[1], Jingfeng Lan[1], Zhigang Xu[1], Tong Chen[1], Tong Zhao[1], Ting Cheng[1], Jianmin Shen[2], Shuangyu Lv[2], & Haixia Zhang[1]

[1]*Key Laboratory of Nonferrous Metal Chemistry and Resources Utilization of Gansu Province, Lanzhou University, Lanzhou 730000, China and* [2]*Institute of Biochemistry and Molecular Biology, School of Life Sciences, Lanzhou University, Lanzhou 730000, China*

Abstract

In the present study, ZnS and ZnO quantum dots (QDs) were synthesized via an all-aqueous process with polyethylene glycol (PEG) chains on their surface, and their toxicity as well as biodistribution were evaluated. No haemolysis occurred at a high concentration of 1600 μg/mL *in vitro* haemolytic assay, which demonstrated that the QDs-PEG displayed good blood compatibility. Following intravenous administration at 2, 6, and 20 mg/kg of the QDs-PEG in mice, the biodistribution, excretion and biocompatibility were characterized at 1 h, 24 h and 7 days, respectively. Quantitative analysis results indicated that the biodistribution trend of ZnS QDs-PEG was similar to that of ZnO QDs-PEG. The QDs-PEG were mainly trapped in the lung and liver, and almost removed from blood within 1 h. QDs-PEG were primarily excreted in faeces at the 2 and 6 mg/kg doses. Coefficients, haematology, blood biochemistry and histopathology results indicated that the QDs-PEG were safe and biocompatible.

Keywords: ZnS QDs, ZnO QDs, haemolysis, biodistribution, toxicity

Introduction

Semiconductor quantum dots (QDs) with specific fluorescence properties, such as size- and composition-tunable emission wavelength, broadband excitation spectrum and photostability, are potential useful tools for imaging, drug delivery systems and other biomedical applications (Geys et al. 2008; Kato et al. 2010; Li et al. 2011b; Lin et al. 2008; Ma et al. 2010; Su et al. 2011). Coupled with specific bioactive moieties (e.g. peptides, antibodies, small molecules, etc.), QDs can also be used as high-performance imaging and diagnostic probes in both *in vivo* and *in vitro* systems (Schipper et al. 2009; Yang et al. 2007). The most recent commercially available and synthesized QDs (e.g. CdSe and CdTe) have been shown to have toxicity and potentially release toxic elements, which could limit their clinical application (Li et al. 2009; Liu et al. 2011b). Thus, minimizing the toxicity of QDs is still a great challenge for their future biological and medical applications. Although various coatings (e.g. ZnS shell and polyethylene glycol (PEG)) have been used to modify the QDs with toxic element, their cytotoxicity can only be partially alleviated, but not completely eliminated (Li et al. 2009). Therefore, a series of QDs without toxic elements, such as ZnS and ZnO QDs, have been developed. ZnS and ZnO QDs are thought to be less toxic than other QDs as Zn is an essential biological element (Yuan et al. 2010). It should be noted that tissue fluorescence interferes with the luminescence of ZnS and ZnO QDs (λ_{em} = 448 nm and λ_{em} = 524 nm). Therefore, more research is needed before they can be used in biomedical application.

It is not fully understood whether QDs may have adverse effects on human health (Li et al. 2011b). As we all know, nanoparticles of decreasing of size may have properties which do not existed in their microparticles (Li et al. 2011a). Accordingly, ZnS and ZnO QDs need to be examined to ensure their safety and biocompatibility before being used for imaging and drug delivery. Only a few relevant studies have been carried out to date. Li et al. (2011b) demonstrated that ZnS QDs did not alter the viability of human endothelial cells (EA hy926), and chitosan-coated ZnS QDs showed low cytotoxicity and good biocompatibility in PANC-1 cells (Chang et al. 2011). ZnO nanoparticles have been reported to induce cytotoxicity *in vitro* and histopathological lesions *in vivo* (Li et al. 2011a), and ZnO QDs have antibacterial activity (Joshi et al. 2009; Jin et al. 2009). However, *in vitro* cultures cannot fully replicate the complexity of the living system or provide meaningful data regarding the response of the physiological system to exogenous agents (Hauck et al. 2010; Phalen et al. 2006). Additionally, there have been no reports on the behaviour of ZnS and ZnO QDs in any animal models, which is preferred for the toxicological assessment of a novel agent (Hauck et al. 2010).

Correspondence: Haixia Zhang, PhD, Key Laboratory of Nonferrous Metal Chemistry and Resources Utilization of Gansu Province, Lanzhou University, 222 Tianshui South Road, Lanzhou 730000, China. Tel: +86 931 8912510. Fax: +86 931 8912582. E-mail: zhanghx@lzu.edu.cn

(Received 19 February 2012; accepted 14 December 2012)

Most biomedical applications require water-dispersible materials, however, numerous QDs are synthesized using organometallic methods (Owens et al. 2011; Su et al. 2011). Thus, following synthesis hydrophobic QDs need additional surface modification to improve their hydrophilicity and biocompatibility (Lee et al. 2010). In the present study, we used environmentally friendly aqueous synthetic strategies to obtain water-stable ZnS and ZnO QDs. Furthermore, the QDs were modified with biologically compatible PEG, which can increase the circulation times of QDs and efficiently avoid nonspecific accumulation *in vivo* (Huang et al. 2011; Schipper et al. 2009; Yang et al. 2007). To provide clearer pharmacokinetic profiles of the QDs-PEG in mice and avoid the complication of the absorption phase, the intravenous route was chosen (Yang et al. 2007). Biodistribution, clearance and excretion of aqueous synthesized QDs-PEG were quantitatively analysed by determination of zinc content. Moreover, coefficients of organs to body weight, haematological characteristics, blood biochemical parameters and histopathological changes were investigated.

Materials and methods

Materials

$ZnSO_4 \cdot 7H_2O$, $Na_2S \cdot 9H_2O$, KOH and ethanol were supplied by Tianjin Guangfu Chemical Reagent Co. Ltd. (China). N,N-dimethylformamide (DMF) was purchased from Tianjin Chemical Reagent Co. Ltd. (China). 1-Ethyl-3-(3-dimethylaminopropyl) carbodiimide hydrochloride (EDC·HCl) was supplied by Shanghai GL Biochem Reagent Co. Ltd. (China). Thioglycolic acid and $ZnAc_2 \cdot 2H_2O$ were purchased from Sinopharm Chemical Reagent Co. Ltd. (Shanghai, China). Polyethylene glycol (PEG, Mw 2000) was purchased from Alfa aesar (Tianjin, China). Dimethylaminopyridine (DMAP), haematoxylin, and eosin were obtained from Sigma (St. Louis, MO, USA). Zinc standard (GSB 04-1761-2004) was purchased from National Center of Analysis and Testing for Nonferrous Metals and Electronic Materials (Beijing, China). Deionized water was prepared from Millipore (Bedford, MA, USA). Other reagents used were of analytical grade. All the QDs-PEG solutions used in this study were fresh prepared.

Synthesis and characterization of water-stable quantum dots

ZnS QDs was prepared using a previously reported method (Wang et al. 2009) with slight modifications. Briefly, 12.5 mmol of $ZnSO_4$ and 40 mL of deionized water were stirred at room temperature (approximately 25°C) for 10 min, and 10 mL of aqueous solution containing 12.5 mmol of Na_2S was added dropwise to the above solution. After stirring for a further 30 min, the product, ZnS QDs was centrifuged (10,280 *g*, 10 min, H-2050 R, Xiang Yi, China) and washed three times with deionized water. The QDs were transferred to a two-necked flask under nitrogen protection, and 10 mL of 0.625 mmol thioglycolic acid in ethanol was added dropwise under vigorous stirring. After 20 h of stirring, the obtained ZnS QDs-COOH were centrifuged (10,280 *g*, 10 min) and dispersed in DMF, to which PEG (1.5 mmol), EDC·HCl (0.938 mmol) and DMAP (0.156 mmol) were added. The mixture was stirred at 0°C for the first 2 h and then at room temperature for 24 h. The resulting ZnS QDs-PEG was centrifuged (10,280 *g*, 10 min) and washed with deionized water and absolute ethanol three times and dried in vacuum.

ZnO QDs was synthesized according to a previously reported method (Patra et al. 2009). Typically, 0.1 mol/L $ZnAc_2$ and 0.2 mol/L KOH solution in ethanol were prepared separately. The reaction was carried out at room temperature by consecutive dropwise addition of 450 mL KOH solution to 150 mL of $ZnAc_2$ solution with stirring. The resulting solution was stirred for a further hour. The obtained ZnO QDs was centrifuged and washed with absolute ethanol three times to neutral. The ZnO QDs was concentrated to ~ 30 mL and transferred to a two-necked flask, in which 10 mL of 0.75 mmol thioglycolic acid in ethanol was added dropwise under nitrogen protection with stirring. After another 20 h of stirring, the resultant mixture (ZnO QDs-COOH) was centrifuged and dispersed in DMF. The subsequent reaction with PEG was the same as that described for the preparation of ZnS QDs-PEG.

Transmission electron microscopy (TEM) images were measured with a TecnaiG^2 F30 (FEI, USA). Absorption spectra were recorded using a Puxi TU-1810 visible spectrophotometer (Beijing, China). Fluorescence spectra were recorded on a RF-5301PC fluorescence spectrometer (Shimadzu, Japan). Large-angle powder X-ray diffraction (XRD) spectra were recorded with a D/max-2400 (Rigaku, Japan) using Cu Kα radiation. The size distribution was determined by dynamic light scattering (DLS) using a BI-200SM (Brookhaven, USA). Fourier transform infrared (FTIR) spectra were carried on a NEXUS 670 FTIR spectrometer (Nicolet, USA). Zeta potentials were recorded on a Zetasizer Nano 3600 (Malvern, U.K.). The Zn contents were measured using flame atomic absorption spectrophotometry (FAAS, AA-6800, Shimazu, Japan). Thermogravimetric analyses (TGA) were performed on a STA PT 1600 (Linseis, Germany) at temperatures ranging from ambient to 800°C under nitrogen.

Haemolysis assay

Human blood samples stabilized by ethylenediamine tetraacetic acid (EDTA) were obtained from Gansu Blood Center (China). Firstly, 2 mL of blood samples was centrifuged at 1260 *g* for 10 min and the red blood cells (RBCs) were isolated from serum. The RBCs were washed five times with 8 mL normal physiological saline (NS, 0.9%) by centrifugation. The purified RBCs were diluted to a 10-fold volume to ensure the absorbance value of the positive control supernatant was in the range of 0.50−0.60 at 576 nm. The RBCs were incubated with deionized water as positive (+) and NS as negative controls (−). Then 0.3 mL of diluted RBCs suspension was added to 1.2 mL NS samples of the QDs-PEG at final concentrations of 100, 200, 400, 800, and 1600 μg/mL. The mixture was shaken gently and then kept in static conditions at room temperature for 3 h. Finally, the mixtures were centrifuged, and the absorbance values of the

supernatants at 576 nm were obtained. The experiments were repeated three times and the percent haemolysis of RBCs was calculated using the following formula [1]:

$$\text{Haemolysis}\,\% = \frac{\begin{array}{c}(\text{Sample absorbances} - \\ \text{negative control absorbance})\end{array}}{\begin{array}{c}\text{positive control absorbances} - \\ \text{negative control absorbance}\end{array}} \times 100\% \quad (1)$$

Animals and treatment

Male Kunming mice of 5–7 weeks old (24–28 g) were supplied by the Experimental Animal Center of Lanzhou University (Lanzhou, China). The animals were housed (5–6/cage) at 22 ± 1°C and 50–60% relative humidity with free access to food and water, under a 12 h light–dark cycle (light on 8:30 a.m. to 8:30 p.m.). All experiments were carried out according to the protocols approved by the Ethics Committee of Animal Experiments of Lanzhou University.

Animals were randomly divided into seven groups (n = 18): a control group and six sample groups (2, 6, and 20 mg/kg of ZnS QDs-PEG, and 2, 6, and 20 mg/kg of ZnO QDs-PEG). The QDs-PEG were sterilized by UV irradiation for 2 h (Liu et al. 2011a) before being suspended in NS and then injected into the tail vein. Six mice from each group were weighed and sacrificed at fixed time points (1 h, 24 h, and 7 days). For haematology and biochemistry analysis, blood was collected using a standard vein blood collection technique before sacrifice. Special single-mouse metabolic cages were used to collect the urine and faeces for a 24 h period prior to sacrifice. Liver, lung, spleen and kidney samples were excised and weighed. A piece of tissue (~ 0.5 × 0.5 × 0.3 cm) was immediately fixed in 10% neutral buffered formalin for further histopathological diagnosis. All the collected biological samples were stored at −20°C for analysis of Zn content. The coefficients of organs were calculated using the following formula [2]:

$$\text{Coefficients of organs} = \frac{\text{Mass of tissues(mg)}}{\text{Mass of body weight (g)}} \quad (2)$$

Quantitative analysis of Zn contents by FAAS

The collected urine, faeces, blood and organs (about 50 mg) were digested with 1 mL of 70% nitric acid at 90°C for 3 h, 0.1 mL perchloric acid was added and then heated for another half an hour. The digested solution was diluted to 5 mL with deionized H_2O for Zn content quantification. The percent of injected dose per gram tissue (% ID/g) and per organ (% ID/organ) of QDs-PEG in a specific tissue were calculated using the following equations [4] and [5]:

$$[\text{Zn}]_{\text{tissue}}(\mu\text{g}/\text{g}) = \frac{[\text{Zn}]_{\text{tissue suspention}} \times 5\text{mL}}{\text{wet weight of tissue}} \quad (3)$$

$$\%\ \text{ID}\Big/\text{g} = \frac{[\text{Zn}]_{\text{treated tissue}} - [\text{Zn}]_{\text{average control tissue}}}{\text{total weight of injected Zn}} \times 100\% \quad (4)$$

$$\%\text{ID}/\text{organ} = \frac{\left\{[\text{Zn}]_{\text{treated tissue}} - [\text{Zn}]_{\text{average control tissue}}\right\} \times \text{total weight of organ}}{\text{total weight of injected Zn}} \times 100\% \quad (5)$$

Haematology analysis and blood biochemical assays

Twenty microlitres of fresh blood was diluted and analysed using a haematology autoanalyzer (BC-3000, MaiRui, China). Red blood cell count (RBC), haemoglobin (HGB), haematocrit (HCT), mean corpuscular volume (MCV), mean corpuscular haemoglobin (MCH), mean corpuscular haemoglobin concentration (MCHC), platelet count (PLT) and white blood cell count (WBC) were determined. 0.8 mL blood samples were centrifuged at 1260 g for 10 min to obtain serum, which was stored at −20°C until measurement. The blood biochemical markers were analysed by a biochemical autoanalyzer (Accute 400, Toshiba, Japan). The serum levels of alanine aminotransferase (ALT), aspartate aminotransferase (AST), total bilirubin levels (TBIL), alkaline phosphatase (ALP) and albumin (ALB) were examined to determine for liver function. Blood urea nitrogen (BUN) and creatinine (CREA) were assessed to identify nephrotoxicity. Lactate dehydrogenase (LDH) was examined to evaluate damage to multiple tissues.

Histopathological examinations

The organ samples (~ 0.5 × 0.5 × 0.3 cm) were fixed in 10% neutral buffered formalin for 24 h, dehydrated progressively in concentrated ethanol to remove water, cleared in xylene to remove ethanol, and finally embedded in paraffin blocks. Five-μm sections were cut and then stained with haematoxylin and eosin (H & E) for histological examination. After H & E staining, the morphology of the tissue on slides was observed under an optical microscope (EX30, Sunny, China).

Statistical analysis

All the data are presented as mean ± S.E.M. Multiple group comparisons of the means were evaluated by one-way analysis of variance (ANOVA) using SPSS 16.0 and $p < 0.05$ was considered statistically significant.

Results

Characterization of aqueous synthesized quantum dots

The single crystal structures of ZnS and ZnO QDs are shown in the TEM micrograph (Figure 1). The average diameter of ZnS and ZnO QDs were approximately 4.2 and 5.4 nm, respectively, which were consistent with the data from DLS measurements (Figure 2D (a) and (c)). The sizes of PEG-modified QDs were 85.2 and 94.0 nm for ZnS and ZnO (Figure 2D (b) and (d)), respectively.

The UV–Vis absorption and photoluminescence (PL) spectra of ZnS and ZnO QDs (blue lines) and the QDs-PEG (red lines) are shown in Figure 2A and B. Following PEG

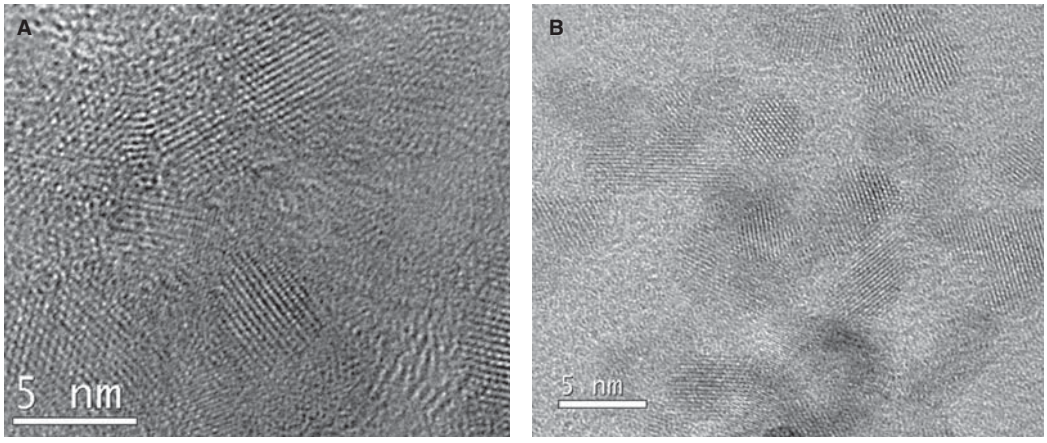

Figure 1. TEM images of (A) ZnS and (B) ZnO QDs.

modification, no obvious change occurred in the absorbance curves. The emission peak showed a small red shift for ZnS QDs, but not for ZnO QDs.

The diffraction peaks of the XRD spectra of ZnS QDs (Figure 2C (a)) corresponded to (111), (220), and (311), which indicated a typical cubic structure. The intensities of the ZnS QDs-PEG (Figure 2C (b)) diffraction peaks were weaker than those of pure ZnS QDs, which demonstrated the presence of amorphous PEG on the surface of ZnS QDs. Similarly, the diffraction peaks of the XRD spectra of ZnO QDs (Figure 2C (c)) corresponded to (100), (002), (101), (102), (110), (103), and (200) planes, which indicated a

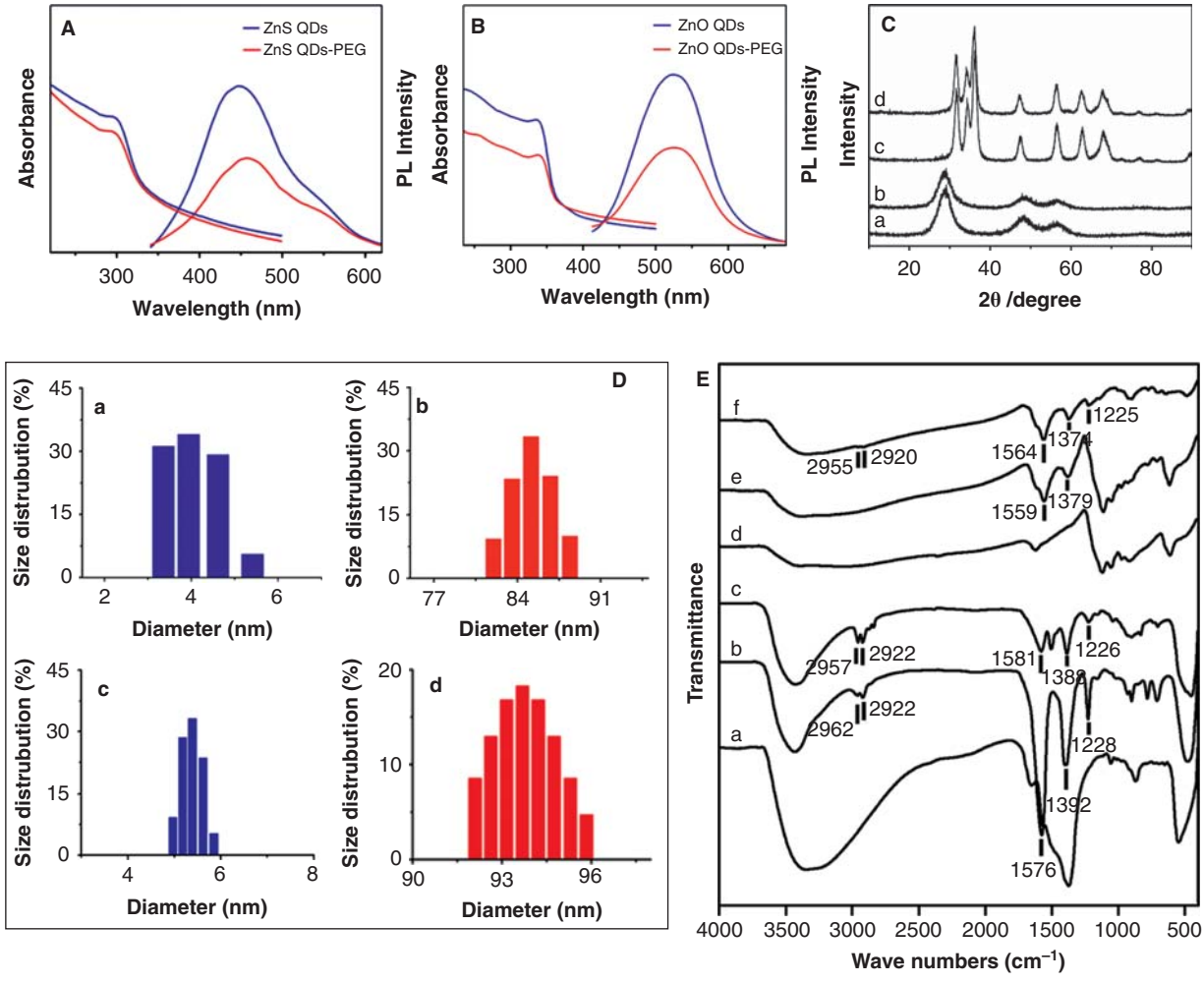

Figure 2. Characterization of aqueous synthesized quantum dots. (A) UV–Vis absorption and photoluminescence (PL) spectra of ZnS QDs and ZnS QDs-PEG. (B) UV–Vis and PL spectra of ZnO QDs and ZnO QDs-PEG. (C) XRD patterns of (a) ZnS QDs, (b) ZnS QDs-PEG, (c) ZnO QDs, and (d) ZnO QDs-PEG. (D) The size distribution of (a) ZnS QDs, (b) ZnS QDs-PEG, (c) ZnO QDs, and (d) ZnO QDs-PEG. (E) FTIR spectra of (a) ZnO QDs, (b) ZnO QDs-COOH, (c) ZnO QDs-PEG, (d) ZnS QDs, (e) ZnS QDs-COOH, and (f) ZnS QDs-PEG.

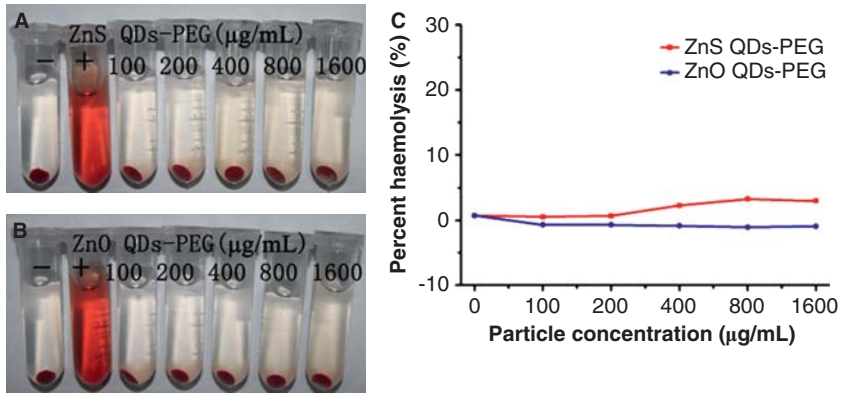

Figure 3. Photograph of RBCs haemolysis assay incubated with different concentrations of (A) ZnS and (B) ZnO QDs-PEG from 100 to 1600 μg/mL using deionized water and normal physiological saline as the positive (+) and negative controls (−). Percent haemolysis of ZnS (red) and ZnO QDs-PEG (blue) (C). Data represent the mean ± S.E.M. from three independent experiments.

hexagonal structure. A decrease in the intensities of the diffraction peaks for ZnO QDs-PEG was also observed (Figure 2C (d)).

The FTIR spectra shown in Figure 2E were used to determine the successful modification of PEG. The FTIR spectra of (a) and (d) corresponded to the pure ZnO and ZnS QDs, respectively. The FTIR spectrum of the ZnO QDs-COOH (b) showed the characteristic peak at 1576 cm^{-1} (C=O stretching vibration) and two weak peaks at 2922 cm^{-1} and 1392 cm^{-1} (the stretching and bending vibration of methylene groups), which were absent in pure ZnO QDs (a). The peak appeared at 1581 cm^{-1} in the FTIR spectrum of ZnO QDs-PEG (c) was associated with ester groups, which demonstrated the successful synthesis of PEG. The new peaks at 1559 cm^{-1} and 1379 cm^{-1} in the FTIR spectrum of ZnS QDs-COOH (e), suggested a successful reaction between ZnS QDs and thioglycolic acid. The absorption peak at 1564 cm^{-1} in the FTIR spectrum of ZnS QDs-PEG (f) indicated the successful conjugation of PEG and ZnS QDs-COOH.

Zeta potential was measured to investigate the charge on the surface of the materials. The results showed that the zeta potential decreased from 12.0 mV (ZnS QDs) to 6.46 mV

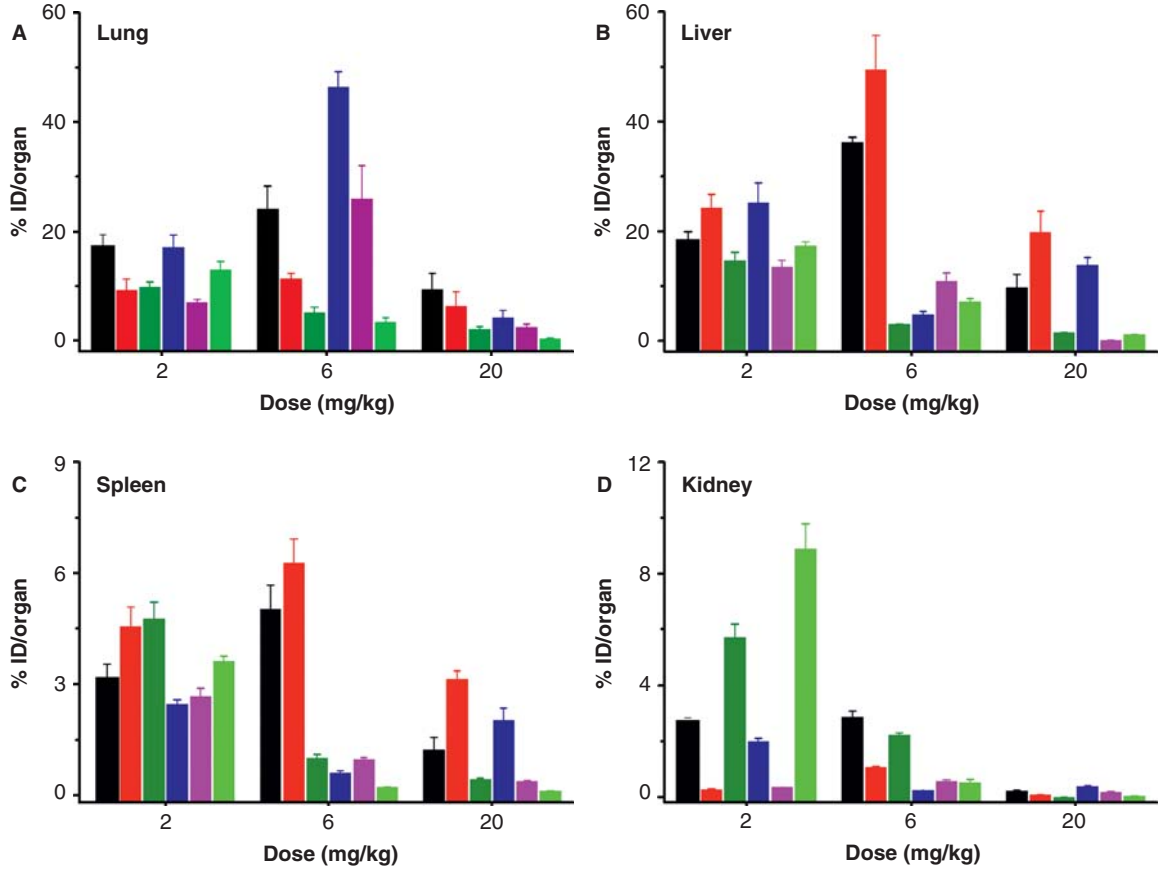

Figure 4. Biodistribution of ZnS and ZnO QDs-PEG with the 2, 6, and 20 mg/kg doses at different time points in (A) lung, (B) liver, (C) spleen, and (D) kidney. ZnS QDs-PEG 1 h, ZnS QDs-PEG 24 h, ZnS QDs-PEG 7 days, ZnO QDs-PEG 1 h, ZnO QDs-PEG 24 h, ZnO QDs-PEG 7 days. All data are presented as mean ± S.E.M. ($n = 6$).

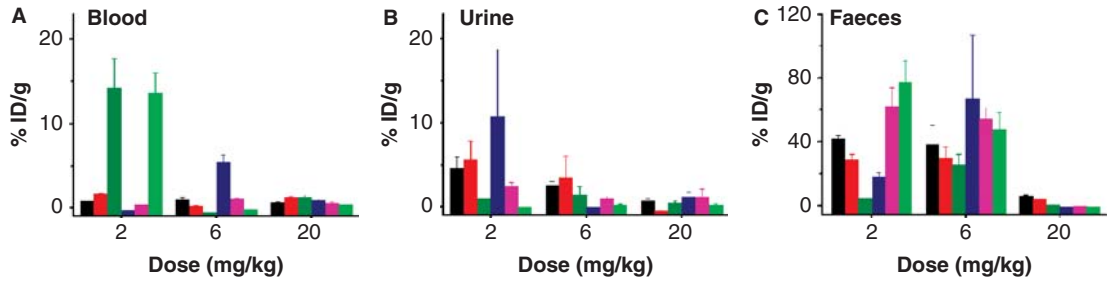

Figure 5. Quantitative analysis of Zn content in (A) blood, (B) urine, and (C) faeces with different doses of ZnS and ZnO QDs-PEG at 1 h, 24 h, and 7 days. ZnS QDs-PEG 1 h, ZnS QDs-PEG 24 h, ZnS QDs-PEG 7 days, ZnO QDs-PEG 1 h, ZnO QDs-PEG 24 h, ZnO QDs-PEG 7 days. All data are presented as mean ± S.E.M. (n = 6).

(ZnS QDs-PEG) and from 21.1 mV (ZnO QDs) to 10.4 mV (ZnO QDs-PEG), indicating the successful synthesis of the QDs-PEG.

The Zn contents were found to be 56.8% in ZnS QDs-PEG and 64.1% in ZnO QDs-PEG using FAAS. The percent of PEG on the surface of QDs was 19.40% for ZnS and 15.29% for ZnO using TGA.

Haemolysis assays

The haemolytic activity of the QDs-PEG on human RBCs was evaluated. From the images in Figure 3A and B, no apparent haemolysis occurred in the ZnS or ZnO QDs-PEG-treated groups within the experimental concentration range, while the positive control (+) solution was red indicating haemoglobin release from damaged RBCs. Even at high concentration (1600 μg/mL, Figure 3C), the percentage of haemolysis caused by QDs-PEG were only 3.00% for ZnS and −0.90% for ZnO.

Quantitative analysis of Zn contents

The Zn contents in biological samples from the control and from mice treated with the QDs-PEG were measured using atomic absorption spectrometry, and the method is shown in supporting information. The basal Zn level in each organ in the control was 18.54 ± 1.78 μg/g for lung, 28.49 ± 1.17 μg/g for liver, 20.39 ± 1.72 μg/g for spleen, and 21.01 ± 0.60 μg/g for kidney. The basal Zn contents were 5.68 ± 0.75 μg/g for blood, 2.02 ± 0.12 μg/g for urine, and 125.98 ± 10.22 μg/g for faeces.

Figure 4 shows the biodistribution of Zn content in representative organs. It was found that Zn was mainly accumulated in the lung and liver. At the low dose of 2 mg/kg QDs-PEG, Zn levels were relatively stable in the reticuloendothelial system (RES) of lung, spleen, and liver at 1 h, 24 h, and 7 days after administration, while the observed fluctuation in biodistribution with time was larger for the 6 mg/kg QDs-PEG dose. At the dose of 20 mg/kg, accumulation of Zn in the organs was very low after 1 week. The clearance rate of ZnO QDs-PEG was much quicker than ZnS QDs-PEG at 20 mg/kg, especially in the liver and spleen.

The Zn levels in lung (Figure 4A) reached the peak at 1 h. Especial for the dose of 6 mg/kg, the highest zinc content was 24.2 ± 4.1% ID/organ for ZnS QDs-PEG and 46.5 ± 2.8% ID/organ for ZnO QDs-PEG. The biodistribution of ZnS QDs-PEG in liver (Figure 4B) almost peaked at 24 h, which was 49.5 ± 6.3% ID/organ for the dose of 6 mg/kg. The biodistribution trend of ZnO QDs-PEG in the liver was different for each dose. At the dose of 20 mg/kg, the accumulated Zn content in the liver reached 13.8 ± 1.4% ID/organ, but returned to baseline 1 day later. The biodistribution and clearance of the QDs-PEG in spleen (Figure 4C) were similar to those in the liver. It should be noted that for the dose of 2 mg/kg, the biodistribution percentages in the kidney (Figure 4D) reached 2.8 ± 0.1% ID/organ for ZnS QDs-PEG and 2.0 ± 0.1% ID/organ for ZnO QDs-PEG at 1 h, decreased to the control level, and then increased to a higher level (5.7 ± 0.5% ID/organ for ZnS QDs-PEG and 8.9 ± 0.9% ID/organ for ZnO QDs-PEG) again at 7 days.

Figure 5A shows the pharmacokinetic processes in blood. The QDs-PEG had a circulation lifetime of less than 1 h, with the exception of ZnO QDs-PEG at the 6 mg/kg dose (5.5 ± 0.8% ID/g). Surprisingly, the Zn contents in blood sharply increased at 7 days for the 2 mg/kg dose (14.2 ± 3.5% ID/g for ZnS QDs-PEG and 13.6 ± 2.4% ID/g for ZnO QDs-PEG). Zn content was detected in urine after the QDs-PEG injected at 1 h (Figure 5B), and the percentage of excretion decreased with increased dose. In the faeces samples, numerous QDs-PEG were excreted at the 2 and 6 mg/kg doses, while the quantity excreted following the 20 mg/kg dose was similar to the control level (Figure 5C).

Coefficients of organs

Daily behaviours such as eating, drinking and activity in the QDs-PEG-treated groups were the same as the control group. Table I shows the coefficients of lung, liver, spleen, and kidney which were not influenced 24 h after injection of QDs-PEG. Compared with the control group (4.73 ± 0.22 mg/g), the coefficient of spleen was significantly elevated (8.03 ± 0.79 mg/g, $p < 0.01$) 7 days after intravenous injection of 20 mg/kg ZnO QDs-PEG. The coefficient of liver was decreased after injection of 6 mg/kg QDs-PEG at 7 days (control: 57.41 ± 2.14 mg/g; ZnS QDs-PEG, 50.10 ± 2.40 mg/g; ZnO QDs-PEG, 49.74 ± 2.23 mg/g, respectively), but without statistical significance. The coefficients of lung and kidney showed no significant change 7 days after injection of the QDs-PEG at all dosages.

Haematology, blood biochemical and histopathological analysis

Haematology and blood biochemical indicators were analysed to assess the influence of the QDs-PEG on blood. Representative haematology markers were determined and

Table I. Coefficients of organs to body weight (BW) of mice at 24 h and 7 days after intravenously injected of three doses of ZnS and ZnO QDs-PEG.

		24 h after injection					7 days after injection				
Index	Dose (mg/kg)	BW (g)	Lung (mg/g)	Liver (mg/g)	Spleen (mg/g)	Kidney (mg/g)	BW (g)	Lung (mg/g)	Liver (mg/g)	Spleen (mg/g)	Kidney (mg/g)
Control	–	25.42 ± 0.31	6.89 ± 0.15	55.09 ± 1.45	5.48 ± 0.54	13.46 ± 0.51	28.81 ± 0.75	6.93 ± 0.22	57.41 ± 2.14	4.73 ± 0.22	13.69 ± 0.34
ZnS QDs-PEG	2	24.60 ± 0.81	7.38 ± 0.14	53.40 ± 4.00	4.77 ± 0.36	14.06 ± 0.67	32.78 ± 1.54	6.67 ± 0.25	58.63 ± 0.90	4.59 ± 0.31	13.85 ± 0.76
ZnS QDs-PEG	6	26.65 ± 0.72	7.55 ± 0.26	55.45 ± 2.19	5.98 ± 0.30	13.46 ± 0.91	30.60 ± 0.85	6.97 ± 0.34	50.10 ± 2.40	4.18 ± 0.30	14.14 ± 0.53
ZnS QDs-PEG	20	25.23 ± 0.68	7.16 ± 0.26	52.46 ± 2.54	5.96 ± 0.71	13.36 ± 1.51	29.53 ± 0.47	6.80 ± 0.16	62.00 ± 3.21	4.85 ± 0.31	13.60 ± 0.71
ZnO QDs-PEG	2	25.07 ± 0.38	6.80 ± 0.24	52.37 ± 1.48	4.76 ± 0.37	13.18 ± 0.55	32.10 ± 0.38	6.57 ± 0.08	56.18 ± 2.77	4.36 ± 0.25	14.11 ± 0.72
ZnO QDs-PEG	6	26.63 ± 0.66	7.03 ± 0.24	54.69 ± 1.59	5.74 ± 0.44	12.89 ± 0.50	32.12 ± 0.82	6.64 ± 0.16	49.74 ± 2.23	4.01 ± 0.23	13.84 ± 0.67
ZnO QDs-PEG	20	25.05 ± 0.41	6.96 ± 0.11	54.52 ± 2.70	5.05 ± 0.51	13.02 ± 0.49	28.30 ± 0.76	7.06 ± 0.26	53.75 ± 1.25	8.03 ± 0.79[a]	14.78 ± 0.34

All data are presented as mean ± S.E.M. ($n = 6$); [a]$p < 0.01$ versus control according to ANOVA.

are shown in Figure 6. All the haematology markers were within normal ranges and did not indicate a trend in toxicity associated with time and dosage. The blood biochemical parameters were not significantly different between the control and the QDs-PEG-treated groups (Figure 7). The histological results of representative organs 7 days after injection of 20 mg/kg QDs-PEG are shown in Figure 8, and no obvious histopathological lesions or abnormalities (i.e. tissue damage, inflammation or lesions) were observed.

Discussion

QDs are promising novel materials for drug delivery and biomedical applications. In order to assess their usefulness, *in vivo* behaviour must be characterized, because theoretical inference or *ex vivo* assay alone cannot completely elucidate the safety of novel nanodelivery systems (Schipper et al. 2009). In our study, aqueous synthesized QDs-PEG did not cause significant toxicity *in vitro* haemolysis assay. After intravenous injection to mice, the QDs-PEG mainly accumulated in the lung and liver, were primary excreted through faeces, and had good biocompatibility as seen from the results *in vivo*.

Due to the lack of toxic elements, ZnS and ZnO QDs are more viable imaging and biomedical tools, however, *in vivo* behaviour should be assessed before their application in the biomedical field. After intravenous administration, the first physiological system that materials encounter is blood and blood components (Huang et al. 2011). *In vivo*, haemolysis can lead to anaemia, jaundice and other pathological changes (Dobrovolskaia et al. 2008). Accordingly, the potential haemolysis of all intravenously administered pharmaceuticals should be evaluated. Haemolytic activity *in vivo* can be predicted by evaluating the degree of erythrocyte haemolysis *in vitro*, which is probably the simplest and most reliable assay for estimating blood compatibility of exogenous compounds (Lee et al. 2004). The membrane-damaging properties of the QDs-PEG were determined by quantitation of haemoglobin concentration in the supernatant of the QDs-RBCs mixture. The haemolysis ratios of the QDs-PEG were all under 5%, even at the relatively high concentration of 1600 μg/mL. A previous report showed that negligible haemolysis (<5%) is acceptable for medical applications (Sun et al. 2011).

In vivo, QDs interact with the living environment directly and continuously. Although cytotoxicity of ZnS and ZnO QDs *in vitro* have been reported in the scientific literature (Li et al. 2011a; b; Chang et al. 2011; Joshi et al. 2009; Jin et al. 2009), evaluation of the toxicity and biocompatibility of these QDs *in vivo* is still required. The present study systematically explored the biodistribution, excretion and biocompatibility of ZnS and ZnO QDs-PEG in mice. It is vitally important and necessary to evaluate the biodistribution and excretion of nanomaterials and to identify their passive target capacities prior to future potential bioapplications (He et al. 2011). According to the quantitative analysis results, the QDs-PEG were predominantly trapped in the lung and liver. High accumulation in the lung was consistent with the biodistribution of other QDs in previous reports (Bao et al. 2012; Lee et al. 2010, Salykina et al. 2011). It is worth pointing out

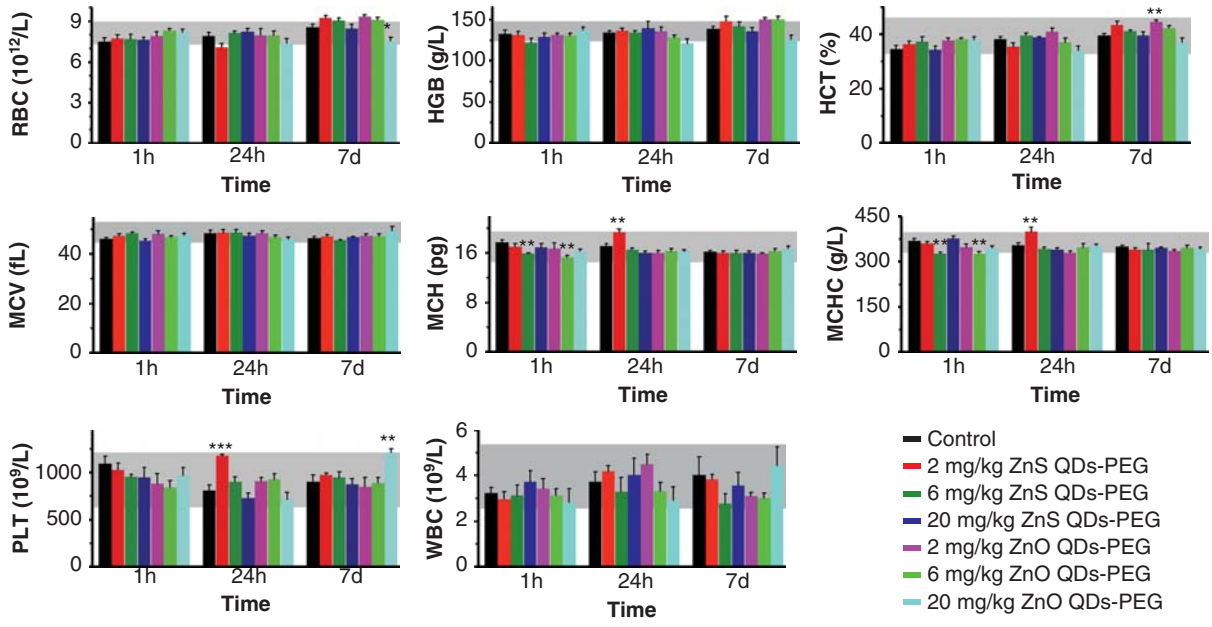

Figure 6. Relative haematology results after injection of ZnS and ZnO QDs-PEG with different concentrations at 1 h, 24 h, and 7 days. Indicators: red blood cell count (RBC), haemoglobin (HGB), haematocrit (HCT), mean corpuscular volume (MCV), mean corpuscular haemoglobin (MCH), mean corpuscular haemoglobin concentration (MCHC), platelet count (PLT) and white blood cell count (WBC). All data are presented as mean ± S.E.M. ($n = 6$). $^{*}p < 0.05$, $^{**}p < 0.01$, and $^{***}p < 0.001$ versus control according to ANOVA.

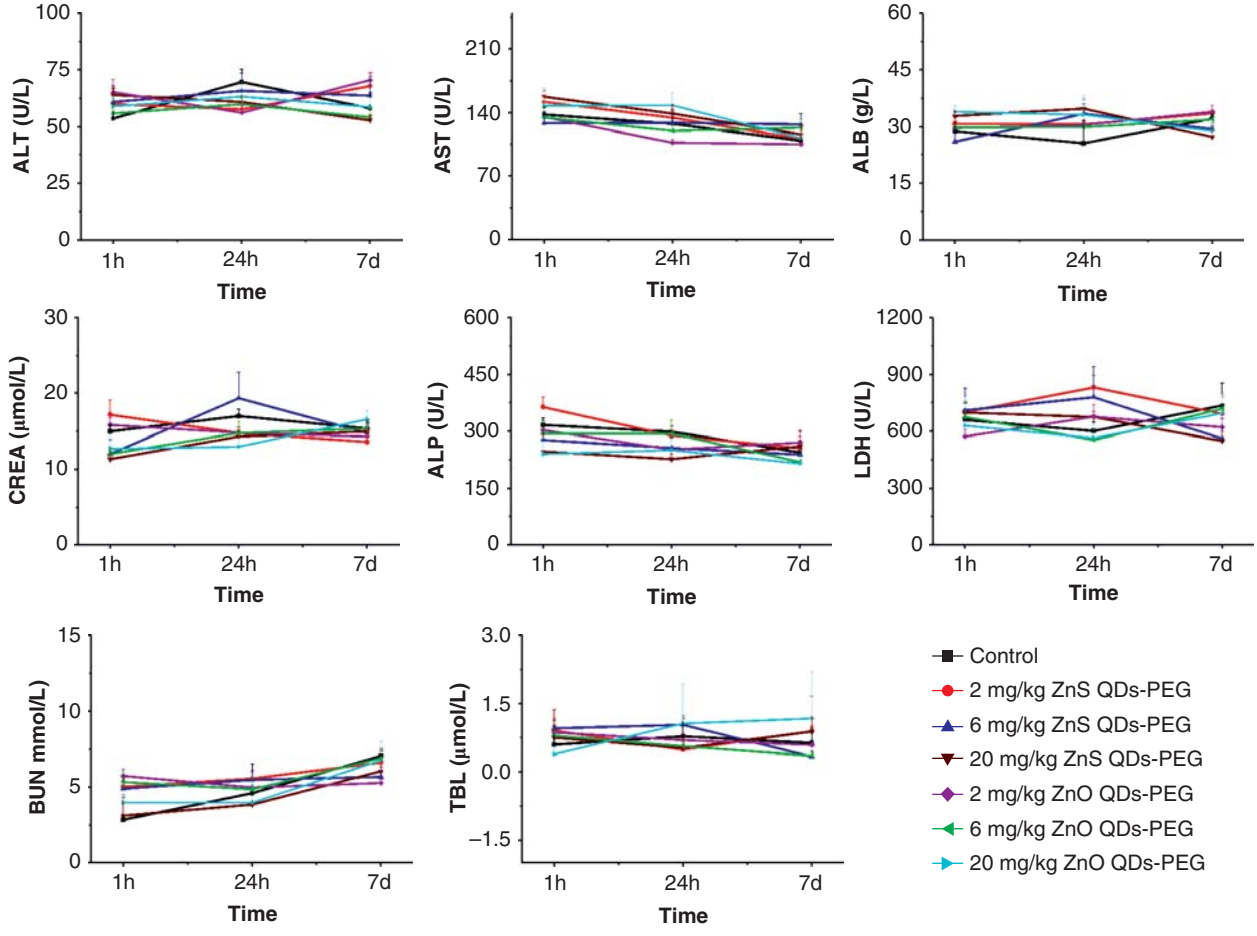

Figure 7. Blood biochemical parameters after injection of ZnS and ZnO QDs-PEG with different concentrations at 1 h, 24 h, and 7 days. Related blood biochemistry indicators: alanine aminotransferase (ALT), aspartate aminotransferase (AST), alkaline phosphatase (ALP), total bilirubin levels (TBIL), urea nitrogen (BUN), creatinine (CREA), lactate dehydrogenase (LDH) and albumin (ALB). All data are presented as mean ± S.E.M. ($n = 6$). No statistically significant changes were observed between QDs treated groups and control according to ANOVA.

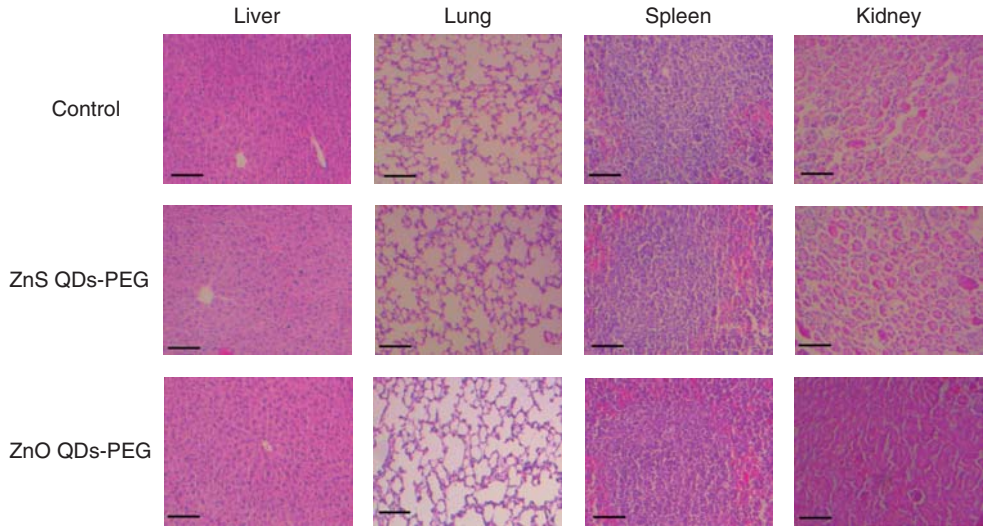

Figure 8. Histopathology of the liver, lung, spleen, and kidney after intravenous injection of 20 mg/kg ZnS and ZnO QDs-PEG at 7 days. The scale bar is 100 μm.

that biodistribution of the QDs-PEG in the spleen after intravenous injection was relatively high owing to the light weight of the spleen. A possible reason for higher Zn content in the reticuloendothelial system (RES) of lung, liver, and spleen is that circulating QDs could be taken by resident phagocytes in these tissues, such as Kupffer cells in the liver, alveolar macrophages in the lung, and macrophages as well as B cells in the spleen (Huang et al. 2011). The ZnS and ZnO QDs-PEG had a comparable biodistribution trend. Accumulation of 2 mg/kg QDs-PEG were relatively stable in lung, liver, and spleen with time, which suggests that the QDs-PEG may be difficult to be removed from the RES organs at this dose. At the dose of 6 mg/kg, the accumulation of ZnO QDs-PEG was higher than that of ZnS QDs-PEG in the lung, but lower in liver, spleen, and kidney. The biodistribution of the QDs-PEG in these organs was low after injection of the 20 mg/kg dose.

The process of opsonization is one of the most important biological barriers in the biomedical applications of nanoparticles, because opsonin proteins present in the blood serum can quickly bind to nanoparticles, allowing macrophages to recognize and remove them from the bloodstream (Owens & Peppas 2006). The QDs-PEG were almost removed from the bloodstream within 1 h. These results were consistent with previous research which showed that QDs were likely to be opsonized by serum proteins and the coating of PEG 2000 increased the blood circulation time of QDs to a maximum of 18 min (Schipper et al. 2009). We also investigated whether the QDs-PEG could be excreted from the body through urine by renal filtration and faeces via hepatic processing and biliary excretion (Huang et al. 2011; Tsoi et al. 2012). Compared with the low Zn contents in urine samples, faeces may be the main excretion pathway for the QDs-PEG.

QDs may induce an inflammatory response, change the activity of the immune system or alter related haematological factors after intravenous injection (Hauck et al. 2010). Haematological parameters are used as an effective and sensitive index to monitor physiological and pathological changes in animals and humans (Duan et al. 2010). None of the relative markers changed after injection of the QDs-PEG, which indicated that the QDs-PEG did not affect haematology. Once the nanoparticles leave the bloodstream and reach the liver and kidneys, it is important to determine whether the particles themselves or their constituent materials can induce toxicity (Hauck et al. 2010). No significant changes in blood biochemical indicators were observed, indicating that the QDs-PEG had no observed adverse effect on liver and kidney function. To further determine possible tissues damage, histological assessments of representative organs, including liver, lung, spleen, and kidney were performed. No apparent histopathological abnormalities or lesions occurred in the QDs-PEG-treated groups compared with the control. These results prove that both ZnS and ZnO QDs-PEG have little systemic toxicity and have great potential for future biomedical applications. The luminescence should be further enhanced to improve the contrast to tissue auto-fluorescence before their use *in vivo*.

Conclusions

In this study, aqueous ZnS and ZnO QDs-PEG were synthesized and their *in vivo* behaviours were characterized. We evaluated both toxicity and biodistribution of the QDs-PEG in mice. The *in vitro* haemolysis assay showed that they had good blood compatibility. After injection, the QDs-PEG were cleared from the blood quickly and accumulated mainly in the lung and liver, and faeces were their major excretion pathway. No apparent abnormalities in haematology, blood biochemistry and histopathology were observed. These results confirmed that the ZnS and ZnO QDs with PEG coating are promising for drug delivery systems and other biomedical applications.

Acknowledgments

This study was supported by the research funds from the State Key Laboratory of Environmental Chemistry and Ecotoxicology, Research Center for Eco-Environmental Sciences, Chinese Academy of Sciences (KF2011-19) and the fund of

Key Laboratory of Chemistry of Northwestern Plant Resources, Lanzhou Institute of Chemical Physics, Chinese Academy of Sciences (CNPR-2012kfkt-10).

Declaration of interest

The authors claim no conflicts of interest. The authors are responsible for the content and writing of the paper.

References

Bao YJ, Li JJ, Wang YT, Yu L, Wang J, Du WJ, et al. 2012. Preparation of water soluble CdSe and CdSe/CdS quantum dots and their uses in imaging of cell and blood capillary. Opt Mater 34(9):1588–1592.

Chang S, Kang B, Dai Y, Zhang H, Chen D. 2011. One-step fabrication of biocompatible chitosan-coated ZnS and ZnS: Mn2+ quantum dots via a γ-radiation route. Nanoscale Res Lett 6(1):591–597.

Dobrovolskaia MA, Clogston JD, Neun BW, Hall JB, Patri AK, McNeil SE. 2008. Method for analysis of nanoparticle hemolytic properties in vitro. Nano Lett 8(8):2180–2187.

Duan Y, Liu J, Ma L, Li N, Liu H, Wang J, et al. 2010. Toxicological characteristics of nanoparticulate anatase titanium dioxide in mice. Biomaterials 31(5):894–899.

Geys J, Nemmar A, Verbeken E, Smolders E, Ratoi M, Hoylaerts MF, et al. 2008. Acute toxicity and prothrombotic effects of quantum dots: impact of surface charge. Environ Health Perspect 116(12):1607–1613.

Hauck TS, Anderson RE, Fischer HC, Newbigging S, Chan WCW. 2010. In vivo quantum-dot toxicity assessment. Small 6(1):138–144.

He Q, Zhang Z, Gao F, Li Y, Shi J. 2011. In vivo biodistribution and urinary excretion of mesoporous silica nanoparticles: effects of particle size and PEGylation. Small 7(2):271–280.

Huang X, Li L, Liu T, Hao N, Liu H, Chen D, et al. 2011. The shape effect of mesoporous silica nanoparticles on biodistribution, clearance and biocompatibility in vivo. ACS Nano 5(7):5390–5399.

Jin T, Sun D, Su J, Zhang H, Sue HJ. 2009. Antimicrobial efficacy of zinc oxide quantum dots against Listeria monocytogenes, Salmonella enteritidis, and Escherichia coli O157: H7. J Food Sci 74(1): M46–M52.

Joshi P, Chakraborti S, Chakrabarti P, Haranath D, Shanker V, Ansari Z, et al. 2009. Role of surface adsorbed anionic species in antibacterial activity of ZnO quantum dots against Escherichia coli. J Nanosci Nanotechnol 9(11):6427–6433.

Kato S, Itoh K, Yaoi T, Tozawa T, Yoshikawa Y, Yasui H, et al. 2010. Organ distribution of quantum dots after intraperitoneal administration, with special reference to area-specific distribution in the brain. Nanotechnology 21(33):335103.

Lee CM, Jang D, Cheong SJ, Kim EM, Jeong MH, Kim SH, et al. 2010. Surface engineering of quantum dots for in vivo imaging. Nanotechnology 21(28):285102.

Lee DW, Powers K, Baney R. 2004. Physicochemical properties and blood compatibility of acylated chitosan nanoparticles. Carbohydr Polym 58(4):371–377.

Li CH, Shen CC, Cheng YW, Huang SH, Wu CC, Kao CC, et al. 2011a. Organ biodistribution, clearance, and genotoxicity of orally administered zinc oxide nanoparticles in mice. Nanotoxicology 6:746–756.

Li H, Li M, Shih WY, Lelkes PI, Shih WH. 2011b. Cytotoxicity tests of water soluble ZnS and CdS quantum dots. J Nanosci Nanotechnol 11 (4):3543–3551.

Li H, Shih WY, Shih WH. 2009. Highly photoluminescent and stable aqueous ZnS quantum dots. Ind Eng Chem Res 49(2):578–582.

Lin P, Chen JW, Chang LW, Wu JP, Redding L, Chang H, et al. 2008. Computational and ultrastructural toxicology of a nanoparticle, Quantum Dot 705, in mice. Environ Sci Technol 42(16):6264–6270.

Liu T, Li L, Teng X, Huang X, Liu H, Chen D, et al. 2011a. Single and repeated dose toxicity of mesoporous hollow silica nanoparticles in intravenously exposed mice. Biomaterials 32(6):1657–1668.

Liu Y, Ai K, Yuan Q, Lu L. 2011b. Fluorescence-enhanced gadolinium-doped zinc oxide quantum dots for magnetic resonance and fluorescence imaging. Biomaterials 32(4):1185–1192.

Ma N, Marshall AF, Gambhir SS, Rao J. 2010. Facile synthesis, silanization, and biodistribution of biocompatible quantum dots. Small 6 (14):1520–1528.

Owens DE 3rd, Peppas NA. 2006. Opsonization, biodistribution, and pharmacokinetics of polymeric nanoparticles. Int J Pharm 307 (1):93–102.

Owens SA, Carpenter MC, Sonne JWH, Miller CA, Renehan JR, Odonkor CA, et al. 2011. Reversed-phase HPLC separation of water-soluble, monolayer-protected quantum dots. J Phys Chem C 115(39):18952–18957.

Patra M, Manoth M, Singh V, Siddaramana Gowd G, Choudhry V, Vadera S, et al. 2009. Synthesis of stable dispersion of ZnO quantum dots in aqueous medium showing visible emission from bluish green to yellow. J Lumin 129(3):320–324.

Phalen RF, Oldham MJ, Nel AE. 2006. Tracheobronchial particle dose considerations for in vitro toxicology studies. Toxicol Sci 92 (1):126–132.

Salykina YF, Zherdeva VV, Dezhurov SV, Wakstein MS, Shirmanova MV, Zagaynova EV, et al. 2011. Biodistribution and clearance of quantum dots in small animals. Proc. SPIE 7999, Saratov Fall Meeting 2010: Optical Technologies in Biophysics and Medicine XII, 799908, doi:10.1117/12.888959.

Schipper ML, Iyer G, Koh AL, Cheng Z, Ebenstein Y, Aharoni A, et al. 2009. Particle size, surface coating, and PEGylation influence the biodistribution of quantum dots in living mice. Small 5(1):126–134.

Su Y, Peng F, Jiang Z, Zhong Y, Lu Y, Jiang X, et al. 2011. In vivo distribution, pharmacokinetics, and toxicity of aqueous synthesized cadmium-containing quantum dots. Biomaterials 32(25):5855–5862.

Sun YN, Wang CD, Zhang XM, Ren L, Tian XH. 2011. Shape dependence of gold nanoparticles on in vivo acute toxicological effects and biodistribution. J Nanosci Nanotechnol 11(2):1210–1216.

Tsoi KM, Dai Q, Alman BA, Chan WC. 2012. Are quantum dots toxic? Exploring the discrepancy between cell culture and animal studies. Acc Chem Res, doi: 10.1021/ar300040z.

Wang HF, He Y, Ji TR, Yan XP. 2009. Surface molecular imprinting on Mn-doped ZnS quantum dots for room-temperature phosphorescence optosensing of pentachlorophenol in water. Anal Chem 81 (4):1615–1621.

Yang RSH, Chang LW, Wu JP, Tsai MH, Wang HJ, Kuo YC, et al. 2007. Persistent tissue kinetics and redistribution of nanoparticles, quantum dot 705, in mice: ICP-MS quantitative assessment. Environ Health Perspect 115(9):1339–1343.

Yuan Q, Hein S, Misra R. 2010. New generation of chitosan-encapsulated ZnO quantum dots loaded with drug: Synthesis, characterization and in vitro drug delivery response. Acta Biomater 6(7):2732–2739.

Supplementary material available online

Supporting information.